

IMPACT OF LI-GRANULE INJECTION ON THE IMPROVEMENT OF BULK ENERGY AND PARTICLE TRANSPORT AND EXPULSION OF MID/HIGH-Z IMPURITIES IN THE LHD HELIOTRON

^{1,*}DANIEL MEDINA-ROQUE, ¹KIERAN J. MCCARTHY, ¹ISABEL GARCÍA-CORTÉS, ²NAOKI TAMURA, ^{3,4}KENJI TANAKA, ⁵FEDERICO NESPOLI, ^{3,6}MAMORU SHOJI, ^{3,6}SUGURU MASUZAKI, ³HISAMICHI FUNABA, ^{3,6}CHIHIRO SUZUKI, ⁵ALBERT MOLLEN, ⁵ROBERT LUNSFORD, ³KATSUMI IDA, ³MIKIRO YOSHINUMA, ^{3,6}MOTOSHI GOTO, ^{3,6}YASUKO KAWAMOTO, ^{3,6}TOMOKO KAWATE, ^{3,6}TOKIHIKO TOKUZAWA, ^{3,6}ICHIHIRO YAMADA AND THE LHD EXPERIMENTAL TEAM.

¹Laboratorio Nacional de Fusión, CIEMAT, Madrid, Spain

²Max-Planck Institute for Plasma Physics, Greifswald, Germany

³National Institute for Fusion Science, National Institutes of Natural Science, Toki, Japan

⁴Interdisciplinary Graduate School of Engineering Sciences, Kyushu University, Kasuga, Japan

⁵Princeton Plasma Physics Laboratory, Princeton, NJ, USA

⁶The Graduate University of Advanced Studies, SOKENDAI, Toki, Japan

Email: daniel.medina@ciemat.es

This study shows, for the first time, simultaneous effective expulsion of mid/high-Z impurities and improvement of bulk energy and particle confinement in high-density and NBI heated plasmas in the Large Helical Device (LHD) by performing continuous lithium (Li) granule injection. In previous studies, impurity accumulation was mitigated through the application of additional ECRH but the concurrent improvement of plasma performance and confinement was not achieved [1, 2].

A major challenge for developing stellarator-based fusion reactors lies in identifying high-density operational regimes that ensure long particle confinement times while minimizing impurity accumulation, particularly for mid/high-Z elements that can trigger plasma radiative collapse. The reduction of the anomalous transport due to plasma turbulence is a standard means to achieve high performance scenarios. However, under these conditions, better confinement of the core impurities is also expected [3]. Here, we investigate the impact of continuous lithium (Li) granule dropping in the LHD on plasma performance and impurity transport. Li granules are found to induce improved plasma confinement and performance, akin to results observed with other low-Z powder injections [4]. Furthermore, high-Z impurities introduced into the plasma core via the Tracer Encapsulated Solid Pellet (TESPEL) method [5] are more effectively expelled, contrary to expectations. In this work we analyze in detail the characteristics of these plasmas and the possible mechanisms responsible for the impurity behavior by SFINCS drift-kinetic transport code simulations [6].

Figure 1 illustrates the heating scheme and key features of the enhanced confinement phase induced by continuous Li granule injection. This phase, beginning at 4.8 s, and continuing until the discharge end (indicated by the Li I signal), is characterized by higher core electron and ion temperatures, increased plasma diamagnetic energy, and a slight rise in line-averaged electron density and effective charge (Z_{eff}). Wall recycling is significantly reduced, as evidenced by the decreased H α signal, leading to improved particle confinement (τ_p), as inferred from the ratio of n_e to H α . This enhanced performance is attributed to reduced ion-scale turbulence across the entire plasma cross-section as measured with two-dimensional phase contrast imaging (2D-PCI) [7]. Figure 2 shows: (a) a substantial reduction in fluctuation amplitude throughout the plasma; (b) fluctuation phase velocities consistent with $\mathbf{E} \times \mathbf{B}$ poloidal rotation velocities, indicating similar radial electric fields (~ 0.4 kV/m at $r/a \approx 0.8$) in both cases; and (c) the temporal

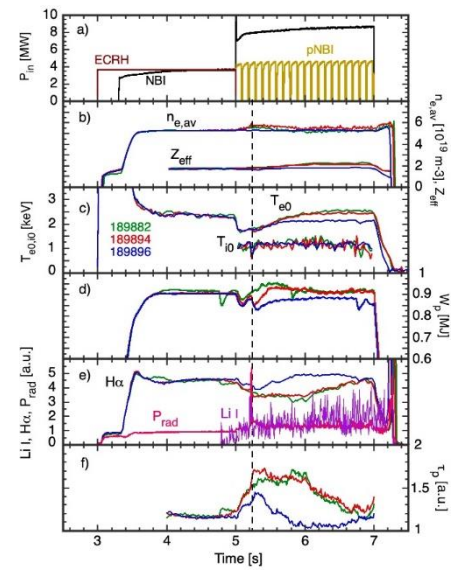
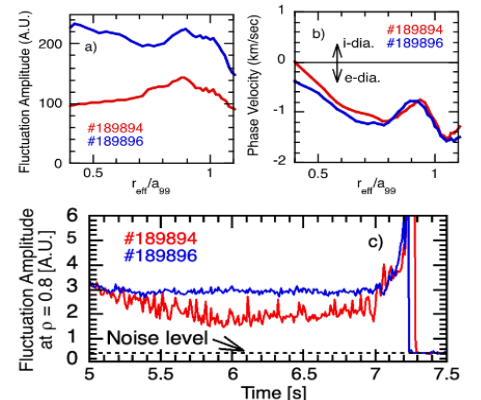


Figure 1. Time traces of a) ECRH, tangential (NBI) and perpendicular (pNBI) neutral beams; b) line-averaged electron density and Z_{eff} c) central T_e and T_i ; d) stored diamagnetic energy, e) Balmer H α (656.3 nm), Li I (670.8 nm) and radiated power emissions, and f) H $^+$ confinement, τ_p , as determined from the ratio n_e to H α , for #189882 (Li-granules only - green), #189894 (Li-granules plus Mo-TESPEL - red) and #189896 (Mo-TESPEL only - blue).



evolution of fluctuation amplitudes at $r/a \approx 0.8$, which closely follows the Li I signal, thereby confirming turbulence suppression due to Li injection.

Mid/high-Z impurity behavior with and without Li granules injection was analyzed by TESPEL injections at 5.225 s during Li-dropping experiments. Spectral emission line evolutions for Ti and Mo (Figure 3) reveal a 28% reduction in Ti confinement time (from ~ 1.47 s to ~ 1.06 s) and a 53% reduction for Mo (from ~ 3.36 s to ~ 1.59 s) with Li-injection compared with reference discharge. Impurity transport simulations using the STRAHL code [8] suggest that these reductions are reproduced by similar values of diffusion coefficient and narrower regions of inward convection velocity (V_{in}) for Ti and lower inward V_{in} for Mo. Moreover, as Er should be very similar in both cases, it should not be the main reason of this reduction of impurity confinement time.

SFINCS drift-kinetic transport code was used to evaluate classical and neoclassical particle transport under reduced turbulence. Results are shown in Fig. 4: (a) neoclassical fluxes for impurity ions (average charge ~ 3.5 to account for He, Li and C was used to reduce the computational costs, which increases with the number of species) become more negative at all radii during reduced turbulence, this enabling low-Z, mainly Li, penetration towards the plasma core, thereby affecting core T_e and T_i as well as turbulence; and (b) total particle fluxes for Mo^{31+} are outwards at all radii for #189896 (no Li-injection) and become more positive outside $r_{eff}/a_{99} \sim 0.45$ for reduced turbulence in #189894 (with Li-injection). These SFINCS fluxes for Mo^{31+} indicate a dominant classical contribution, which is significantly enhanced at $r_{eff}/a_{99} \sim 0.7$ for Li-injection. A possible explanation for the classical transport dominance could be that the diffusive and convective neoclassical terms cancel each other and thus the total neoclassical transport is low for these high-Z elements. Additionally, reduced high-Z impurity confinement aligns quantitatively with the halved inward convective velocity predicted by STRAHL and the doubled outward classical flux calculated by SFINCS.

Finally, with regard to intrinsic impurities (carbon, oxygen, and iron) continuous Li-granule dropping causes a $\sim 30\%$ fall in C III signal, slightly reduced O V signal and an unaffected Fe XVI signal. A cumulative effect of Li deposition on the vacuum chamber walls likely contributes to reduced intrinsic impurity levels in subsequent discharges in addition to a more positive radial electric field (E_r) in the scrape-off layer measured by Doppler reflectometry. These observations point towards an effective impurity screening in plasmas with Li-granule injection.

In summary, continuous Li injection in LHD enhances plasma performance, reduces the plasma turbulence, causes intrinsic impurity screening in the plasma edge and also reduces mid/high-Z impurity confinement times. SFINCS simulation show the dominant role of the neoclassical and the classical channels to explain the behavior of low and high-Z impurities, respectively. These findings highlight the potential of Li-granule injection to improve operational scenarios for stellarators, paving the way for further optimization of fusion reactors.

References:

- [1] N. Tamura et al., Plasma Phys. Control. Fusion 58, 114003 (2016)
- [2] N. Tamura et al., Phys. Plasmas 24, 056118 (2017)
- [3] R. Burhenn et al., Nucl. Fusion 49, 065005 (2009),
- [4] F. Nespoli et al., Nat. Phys. 18, 350 (2022),
- [5] N. Tamura et al., Rev. Sci. Instrum. 87, 11D619 (2016),
- [6] M. Landreman, et al., Phys. Plasmas 21, 042503 (2014),
- [7] K. Tanaka et al., Rev. Sci. Instrum. 74, 1633 (2003),
- [8] K. Berhinger, JET Report, JET-R (87) 08 (1987).

Figure 2 Spatial profiles of (a) fluctuation amplitude, (b) fluctuation phase velocity and (c) time history of fluctuation amplitude at $r_{eff}/a_{99} = 0.8$ as measured using two-dimensional phase contrast imaging (2D-PCI). (#189894 (with Li) and #189896 (without Li)).

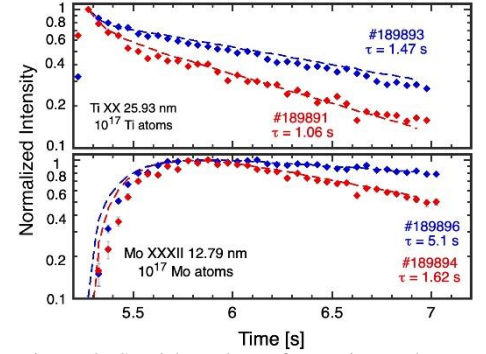


Figure 3. Semi-log plots of experimental tracer spectral line intensities (filled diamonds) and STRAHL predictions (dash lines), normalized to maximum, for discharges #189893 and #189896 (references - blue) plus #189891 and #189894 (Li-granules - red). TESPELs are injected into the latter discharges at 5.225 s. Decay times, τ , are obtained by fits to experimental points

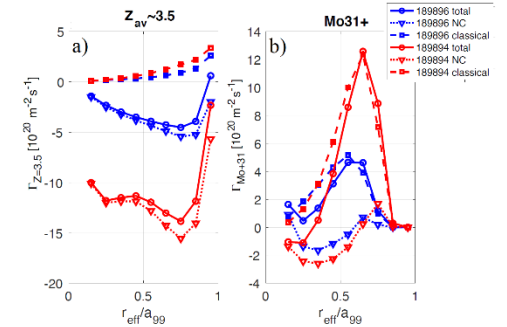


Figure 4. NC (open triangles, short dash-dash), classical (open boxes, long dash-dash) and total (open circles, continuous) particle fluxes normalized to pseudo-densities for a) low-Z tracer with $Z_{average} = \sim 3.5$ and b) trace $Mo+31$, as functions of normalized LHD radius. These are for #189894 (Li-granules - red) and #189896 (reference - blue).